Radiocarbon dating of glacier ice: overview, optimisations, validation and potential

5 Chiara Uglietti[1,2,3], Alexander Zapf[1,2,3†], Theo M. Jenk[1,3], Michael Sigl[1,3], Sönke Szidat[2,3], Gary Salazar[2,3], Margit Schwikowski[1,2,3]

[1]Laboratory of Environmental Chemistry, Paul Scherrer Institute, 5232 Villigen PSI, Switzerland
[2]Department of Chemistry and Biochemistry, University of Bern, 3012 Bern, Switzerland
[3]Oeschger Centre for Climate Change Research, University of Bern, 3012 Bern, Switzerland
10 †deceased

Correspondence to: theo.jenk@psi.ch

Abstract. High altitude glaciers and ice caps from mid-latitudes and tropical regions contain valuable signals of past climatic and environmental conditions as well as human activities, but for a meaningful interpretation this information needs to be placed in a precise chronological context. For dating the upper part of ice cores from such sites several relatively precise 15 methods exist, but they fail in the older and deeper part, where plastic deformation of the ice results in strong annual layer thinning and a non-linear age-depth relationship. If sufficient organic matter such as plant, wood or insect fragments were found, radiocarbon (^{14}C) analysis had thus been the only option for a direct and absolute dating of deeper ice core sections. However such fragments are rarely found and even then very likely not at the depths and in the resolution desired. About 10 years ago, a new, complementary dating tool was therefore introduced by our group. It is based on extracting the µg-amounts 20 of the water-insoluble organic carbon (WIOC) fraction of carbonaceous aerosols embedded in the ice matrix for subsequent ^{14}C dating. Meanwhile this new approach was improved considerably, thereby reducing the measurement time and improving the overall precision. Samples with ~10 µg WIOC mass can now be dated with reasonable uncertainty of around 10-20% (variable depending on sample age). This requires about 300 to 800 g of ice considering the WIOC concentrations typically found in mid- and low-latitude glacier ice. Dating polar ice with satisfactory age precision is still not possible since 25 WIOC concentrations are around one order of magnitude lower. The accuracy of the WIOC ^{14}C method was validated by applying it to independently dated ice. With this method the deepest parts of the ice cores from Colle Gnifetti and Mt. Ortles glacier in the European Alps, Illimani glacier in the Bolivian Andes, Tsambagarav ice cap in the Mongolian Altai, and Belukha glacier in the Siberian Altai have been dated. In all cases a strong annual layer thinning towards bedrock was observed and the oldest ages obtained were in the range of 10000 yrs. WIOC ^{14}C dating was not only crucial for 30 interpretation of the embedded environmental and climatic histories, but additionally gave a better insight into glacier flow dynamics close to bedrock and past glacier coverage. For this the availability of multiple dating points in the deepest parts was essential, which is the strength of the presented WIOC ^{14}C dating method, allowing determination of absolute ages from principally every piece of ice.

Keywords: ice cores, mid- and low latitude glaciers, water-insoluble organic carbon, radiocarbon, chronology

35 **1 Introduction**

High altitude glaciers and ice caps from mid-latitudes and tropical regions contain valuable signals of past climate and atmospheric variability at regional and local scale and are located in areas with large biological diversity and inhabited by the majority of the world's population. Particularly mid-latitudes glaciers, for instance in the European Alps or in the Himalaya, are influenced by the nearby anthropogenic pollution sources, thereby additionally preserving the signature of

40   human activities. This information can generally be retrieved from glacier ice cores, but needs to be placed in a precise chronological context to allow meaningful interpretation with respect to environmental and climatic changes.

Ice core dating is a sophisticated task and the most common approach is annual layer counting, which relies on seasonally fluctuating signals. A number of ice core parameters such as the stable isotope ratio of hydrogen or oxygen in the water (δ^2H, δ^{18}O), the concentration of trace components (e.g. ammonium, mineral-dust-related trace elements, black carbon), and the

45   presence of melt layers may vary with the seasons. To reduce uncertainty in layer counting the time scale is additionally anchored with reference horizons like the radioactivity peak resulting from nuclear weapon tests in the 1960s or tephra and aerosol layers caused by volcanic eruptions(Thompson et al., 1998; Preunkert et al., 2000; Schwikowski, 2004; Eichler et al., 2009; Moore et al., 2012; Thompson et al., 2013). An independent method is nuclear dating with the naturally occurring radioisotope ^{210}Pb. Determined by the ^{210}Pb half-life of 22.3 years and its atmospheric concentration, the time period

50   accessible for dating is in the order of a century (Gäggeler et al., 1983; Eichler et al., 2000; Herren et al., 2013). All these dating techniques fail in the older and deeper part of glaciers, where plastic deformation of the ice, under the weight of the overlying mass, results in horizontal ice flow, stretching annual layers continuously with increasing depth. Correspondingly, the depth-age relationship of high-alpine glaciers is strongly non-linear (Jenk et al., 2009) and annual layers and also volcanic signals become undetectable below a certain depth with the current spatial resolution of most analytical methods.

55   Glacier flow modelling can only give rough age estimates with large uncertainties close to the bedrock of high-alpine glaciers (Lüthi and Funk, 2001). Radiocarbon (^{14}C) analysis has been the only option allowing a direct and absolute dating of these deeper ice core sections in the rare cases when sufficient organic matter such as plant, wood or insect fragments were found (Thompson et al., 1998; Thompson et al., 2002). However, in glacier ice such findings do not only happen very seldomly but even if lucky, they do not allow for continuous or at least regular dating which limits not only the application

60   of the ^{14}C technique but also its use to derive a complete chronology based on absolutely dated layers. In the following we refer to dating of ice with macrofossils as conventional ^{14}C dating.

A new, complementary dating tool was therefore introduced by our group about 10 years ago, which is based on extracting the µg-amounts of the water-insoluble organic carbon fraction of carbonaceous aerosols embedded in the ice matrix for ^{14}C dating (Jenk et al., 2006; Jenk et al., 2007). Carbonaceous compounds represent a large, but highly variable fraction of the

65   atmospheric aerosol mass (Gelencsér, 2004; Hallquist et al., 2009). Total organic carbon (TOC, also referred to as total carbon, TC) is instrumentally divided into two sub-fractions according to their refractory and optical properties. Elemental carbon (EC) consists of highly polymerized substances which are extremely refractory and light absorbent and therefore this fraction is also called black carbon (BC) or soot (Gelencsér, 2004; Hallquist et al., 2009). EC derives merely from the incomplete combustion of fossil fuels and biomass. Organic carbon (OC) is formed by weakly refractory hydrocarbons of

70   low to medium molecular weight. Whereas EC is generally insoluble in water, OC is further subdivided into water-soluble organic carbon (WSOC) and water-insoluble organic carbon (WIOC) (Szidat et al., 2004a). In water samples the former is also known as dissolved organic carbon (DOC) (Legrand et al., 2013; May et al., 2013). OC is emitted directly as primary aerosol from a vast diversity of sources and emission processes, including mobilization of plant debris, pollen, vegetation waxes, microorganisms, spores, the organic fraction of soil as well as emissions from biomass burning (e.g. forest fires) and

75   anthropogenic processes (biomass burning and fossil fuel combustion), but it is also formed in the atmosphere by oxidation of gaseous precursors as secondary organic aerosol (Gelencsér, 2004; Gelencsér et al., 2007; Hallquist et al., 2009).

Carbonaceous aerosols are transported in the atmosphere to high-alpine glaciers, where they may be deposited by both wet and dry deposition processes and finally embedded in glacier ice (Lavanchy et al., 1999; Jenk et al., 2006; Legrand and Puxbaum, 2007; McConnell et al., 2007; Kaspari et al., 2011). Consequently using carbonaceous aerosols allows dating any

80   piece of ice, given that it contains sufficient carbon mass. The WSOC fraction (i.e. DOC) would be ideal for dating, since it has the highest concentrations in ice. However, its extraction is complicated. It involves the outgassing of aqueous atmospheric CO_2, removal of dissolved carbonates, wet oxidation of the organic compounds to CO_2 under inert gas, and

finally quantitative trapping of the evolved CO_2 (May et al., 2013). Since major contributors of DOC, like light carboxylic acids, are ubiquitous in the air, all these steps are prone to contamination. Therefore from the different carbonaceous particle
85 fractions we selected WIOC as target for ^{14}C dating for several reasons. First, WIOC is mainly of biogenic origin in pre-industrial times (Jenk et al., 2006) and therefore supposed to contain a contemporary ^{14}C signal representative of the age of the ice (Jenk et al., 2006; Steier et al., 2006). Second, the average WIOC concentration in ice is higher than the respective EC concentration, allowing for smaller ice samples and potentially higher time resolution, which consequently provides a better signal to noise ratio (mainly determined by the overall blank) and smaller uncertainty of the dating results. Third, OC
90 has a lower probability compared to EC for in-built reservoir ages from e.g. burning of old trees or old organic matter (Gavin, 2001; Sigl et al., 2009). Moreover OC is insensitive to potentially insufficiently removed carbonates in mineral dust rich layers (e.g. Saharan dust), which may contribute to the EC fraction because of the higher combustion temperature applied to EC (Jenk et al., 2006). The extraction of WIOC from the ice is straightforward as it can be collected by filtration of the melted ice. Note that in previous publications (Sigl et al., 2009; Zapf et al., 2013) the term POC was used for
95 particulate organic carbon (Drosg et al., 2007). Since POC can be mistaken with primary organic carbon (Gelencsér, 2004; Zhang et al., 2012) we adopted the term water-insoluble organic carbon (WIOC) instead in this overview.

Our research group has a long history in ^{14}C dating of ice cores using the aforementioned WIOC fraction of carbonaceous particles. Lavanchy et al. (1999) introduced initial methods to determine the concentrations of carbonaceous particles in ice from a European high-alpine glacier. Next, the methodology was developed for source apportionment of aerosols by [14]C
100 measurements in different carbonaceous particle fractions (Szidat et al., 2004b). This was conducted in close collaboration with the Laboratory of Ion Beam Physics of the ETH Zurich, a well established ^{14}C dating facility and a world-leading group in Accelerator Mass Spectrometry (AMS) technology, where simultaneously and continuously the analytical aspect of instrumentation was improved (Synal et al., 2000; Ruff et al., 2007; Synal et al., 2007; Ruff et al., 2010). The methodology of ^{14}C analysis of the different carbonaceous particle fractions was adopted to study the suitability of WIOC for ^{14}C dating of
105 old ice, finding that it is of purely biogenic origin prior to industrialization (Jenk et al., 2006; Jenk et al., 2007). Since then this novel ^{14}C approach has been applied for dating a number of ice cores from different high-altitude mountain glaciers (Table 1), (Jenk et al., 2009; Sigl et al., 2009; Kellerhals et al., 2010; Herren et al., 2013; Zapf et al., 2013; Aizen et al., 2016). Meanwhile the method has been further optimized and was additionally validated by determining the age of independently dated ice. Here we give an overview of the current status of the now routinely applied WIOC ^{14}C dating
110 method for glacier ice, including an update on recent optimizations and method validation. Uncertainties and the potential of this novel approach are discussed and its succesfull application to a number of ice cores presented.

2 Sample preparation, OC/EC separation and ^{14}C analysis

The preparation of ice samples follows the procedure according to Jenk et al. (2007). First, samples are decontaminated in a cold room (-20˚C) by removing the outer layer (3 mm) with a pre-cleaned stainless steel band saw (wiped three times with
115 acetone, followed bycutting of a frozen block of ultra-pure water, 18 MΩ cm quality), followed by rinsing the samples with ultra-pure water in a class 100 clean bench. Around 20-30% of the ice samples' mass is lost during these first steps, resulting in a final mass of about 200 to 500 g (initial mass of around 300-800 g of ice). The samples are then transferred and stored frozen at -20˚C in pre-cleaned (soaked and rinsed for three days with daily exchanged ultra-pure water) 1-L-containers (Semadeni, PETG) until being melted at room temperature directly before filtration. To ensure that carbonates potentially
120 present in the ice are completely dissolved, ~20 mL of 1M HCl (30% Suprapure, Merck) are added to the melted samples (Cao et al., 2013), resulting in a pH of < 2, before being sonicated for 5 min. Subsequently, the insoluble carbonaceous particles are filtered onto preheated (5h at 800˚C) quartz fibre filters (Pallflex Tissuquartz, 2500QAO-UP), using a dedicated glass filtration unit, also carefully pre-cleaned by rinsing with ultra-pure water and by baking the glass at 450˚C for 3h. As a

second carbonate removal step, the filters are acidified three times with a total amount of 50 µL 0.2M HCl (Jenk et al.,
2007). Afterwards the filters are left in a class 100 clean bench for 1h to allow potentially present carbonates to be
transformed into CO_2 by reaction with the HCl, followed by rinsing with 5 ml ultra-pure water to entirely remove remaining
HCl. The filters are left again for 1h to reach complete dryness, packed in aluminium foil and kept frozen until analysis, for
which filters are taken out of the freezer to let them reach ambient temperature (at least half an hour). Details regarding OC
and EC separation, AMS ^{14}C analysis and improvements achieved since the first applications will be discussed in Sections 3
and 4.

3 Recent optimization in OC/EC separation and AMS analysis

In previous ice core dating applications using ^{14}C of WIOC (Jenk et al., 2009; Sigl et al., 2009; Kellerhals et al., 2010;
Herren et al., 2013; Zapf et al., 2013), the OC and EC combustion was performed with the Two-step Heating system for the
EC/OC Determination Of Radiocarbon in the Environment apparatus (THEODORE), developed for aerosol applications
(Szidat et al., 2004b). The combustion was conducted in a stream of oxygen for the controlled separation of OC and EC
fractions. The temperature for OC separation was set at 340˚C, while for recovery of EC the temperature was then increased
to 650˚C. The CO_2 produced by oxidation during the combustion was cryogenically trapped, manometrically quantified and
sealed in glass ampoules (Szidat et al., 2004b). In the earliest application described by Jenk et al. (2006) the CO_2
subsequently had to be transformed to filamentous carbon (graphitisation) using manganese granules and cobalt powder for
final AMS ^{14}C analysis. This was initially performed at the ETH AMS facility (TANDY, 500 kV pelletron compact AMS
system) (Synal et al., 2000). Since 2006, the 200kV compact AMS (MIni radioCArbon DAting System, MICADAS) has
been operational at the ETH (Synal et al., 2007). The MICADAS is equipped with a gas ion source and a Gas Introduction
interface System (GIS) (Ruff et al., 2007; Synal et al., 2007), allowing measurements of ^{14}C directly in CO_2 with an
uncertainty level as low as 1% (Ruff et al., 2010). The GIS includes a gas-tight syringe for the CO_2 injection into the ion
source (Ruff et al., 2010), with a maximum capacity of 1.3 ml of CO_2 as ~5% mixing ratios in helium (equivalent to 100 µg
of carbon). The position of the syringe plunger is automatically adjusted according to the sample size as well as the helium
flow carrying the sample to the ion source. With this, the tranformation of gaseous CO_2 to solid graphite targets became
needless (Sigl et al., 2009). Instead, the glass ampoules sealed after the combustion of the filters with the THEODORE
system were opened in a designated cracker, an integral part of the GIS (Ruff et al., 2007), and the resulting CO_2-He mixture
could directly be fed into the MICADAS ion source.
The main advantages of switching from solid to gaseous targets were: 1. a decrease in the number of necessary preparation
steps and the associated risk of lost samples from incomplete graphitisation, 2. a higher sample throughput, 3. a reduction in
the variability and overall blank contribution as well as 4. the elimination of the correction applied to account for
fractionation during the graphitisation step, which contributed with around 10% to the overall uncertainty (Jenk et al., 2007).
As will be discussed in Section 4, a precision increase is one of the main challenges for improving the method.
Since spring 2013, ^{14}C analysis is performed with a MICADAS installed at the Laboratory for the Analysis of Radiocarbon
with AMS (LARA laboratory) of the University of Bern, also equipped with a GIS interface (Szidat et al., 2014). There, an
improvement was recently achieved by replacing the THEODORE with a commercial combustion system, which is a
thermo-optical OC/EC analyzer (Model4L, Sunset Laboratory Inc., USA), normally used for aerosol OC/EC separation and
source apportionment studies (Zhang et al., 2012; Zhang et al., 2013; Zhang et al., 2014; Zotter et al., 2014). Similar as in the
THEODORE system, the carbonaceous particles are combusted in a stream of pure oxygen. The Sunset instrument is
specially equipped with a non-dispersive infrared (NDIR) cell to quantify the CO_2 produced during the combustion. The
combustion process in the Sunset system follows a well-established protocol (Swiss 4S) for the thermal separation of OC and
EC fractions under controlled conditions (Zhang et al., 2012). To avoid potential damage of the infrared cell detector by

165 residual HCl, the final rinsing of the filters after adding HCl for carbonates removal was introduced (see Section 2)..
Recently the Sunset instrument was directly coupled to the zeolite trap of the GIS (Ruff et al., 2010), which allows online
[14]C measurements of the carbonaceous fractions separated in the Sunset system (Agrios et al., 2015). When combusted, the
gaseous carbonaceous species pass through a MnO_2 bed heated to 850°C for completing the oxidation to CO_2, which is
further transported by helium to the zeolite trap. This trap is then heated up to 500°C to release the CO_2 to the gas-tight

170 syringe for final injection into the AMS ion source (Ruff et al., 2007; Synal et al., 2007).
The newly coupled Sunset-GIS-AMS system has major advantages compared to the old setup. The OC/EC separation in the
THEODORE was relatively time consuming and only four ice samples could be processed per day. Two more days were
needed to produce all the standards and blanks required for AMS calibration and for quality control and graphitisation (Jenk
et al., 2007). Besides the disantvantages of solid graphite targets described before, there is also a risk of losing samples

175 during the delicate phase of flame-sealing the ampoules and later on when scratching them to allow a clean break in the
automated GIS cracker. With the online coupling of the Sunset, this risk is completely removed. Further the preparation and
measurement time is significantly reduced because there is no need for offline combustion resulting in a total measurement
time of approximately 35 min per sample only. In addition, it not only allows for an automated protocol of standard injection
for AMS calibration, but also offers the possibility for easy and regular (daily) survey of the ^{14}C background in the entire

180 process line (Sunset-GIS-AMS) by analysis of variably sized standards and blanks if required (Agrios et al., 2015).). Finally,
the Sunset system enables continuous monitoring of the combustion process, reducing a potential bias due to charring, and
the standardized and automated combustion protocol (Swiss 4S) ensures high reproducibility increasing the overall
precision.
With the current setup, the ^{14}C/^{12}C ratio of the samples is background subtracted, normalized and corrected for mass

185 fractionation by using fossil sodium acetate (^{14}C free, NaOAc, p.a., Merck, Germany), the reference material NIST standard
oxalic acid II (modern, SRM 4990C) and the $\delta^{13}C$ simultaneously measured in the AMS, respectively (Wacker et al., 2010).
All results are expressed as Fraction Modern (F[14]C), which is the ^{14}C/^{12}C ratio of the sample divided by the same ratio of the
modern standard. Further corrections are subsequently applied to the F[14]C values considering isotopic mass balance (e.g.
Jenk et al., 2007) to account for constant contamination, cross contamination and for the procedural blank contribution

190 introduced by the preparation of ice samples (for details see Section 4). [14]C ages (before present (BP), i.e. before 1950) are
calibrated using OxCal v4.2.4 (Bronk Ramsey and Lee, 2013) with the Northern (IntCal13) or Southern Hemisphere
(ShCal13) calibration curves (Hogg et al., 2013; Reimer et al., 2013), depending on the sample site location. Calibrated dates
are given in years before present (cal BP) with 1 σ uncertainty range (Stuiver and Polach, 1977; Mook and van der Plicht,
1999). For simplicity the ages dicussed in the text are given as the mean of this range ±1 σ. See Section 4 for further details

195 regarding the applied corrections, ^{14}C calibration and discussion of uncertainties.
To ensure comparability between previous data and the newly derived results, using the above described improved setup
configuration, ^{14}C analysis was conducted on remaining pieces of samples, which were previously processed with the
THEODORE setup. Two samples (JUV 1 and JUV 3) from the Juvfonne ice patch in Norway (Zapf et al., 2013) and two
samples (BEL 1 and BEL 2) from an ice core drilled at Belukha glacier in the Siberian Altai (Aizen et al., 2016) were used,

200 covering an age range from modern to more than 8000 cal BP. The OC masses were above 10 µg carbon, except for sample
Juv2_Sunset with a carbon mass of 9 µg (Table 2), still resulting in more than 4500 ^{14}C counts with a corresponding
uncertainty of the F[14]C of 2%, which we consider sufficiently low for this comparison. At first, the obtained WIOC
concentrations are discussed, which are assumed to agree as indicated by a carbon quantification test carried out on
homogeneous aerosol filters using both combustion instruments (Zotter et al., 2014). As expected a good consistency was

205 found for the WIOC concentrations in the Belukha ice core (Table 2), whereas a discrepancy was observed for the Juvfonne
samples, probably related to the natural inhomogeneity of particles in this small-scale ice patch with a distinct ice
accumulation behaviour (see below). Concerning the ^{14}C ages, a very good agreement is shown between all parallel samples

(Figure 1). This is also true for the procedural blanks , both in term of carbon amount and $F^{14}C$.. The WIOC procedural blank measured and used for correction in this comparision experiment was 1.41 ± 0.69 µg of carbon with an $F^{14}C$ of 0.64 ± 0.12, and 1.21 ± 0.51 µg of carbon with an $F^{14}C$ of 0.73 ± 0.13 for the THEODORE and the coupled Sunset setup, respectively (additional details can be found in Section 4). In summary, we conclude that dating results obtained with the previously used THEODORE combustion setup (Jenk et al., 2009; Sigl et al., 2009; Herren et al., 2013; Zapf et al., 2013) and the improved coupled Sunset-GIS-AMS system are in good agreement.

4 Radiocarbon dating uncertainties

First of all, the signal-to-noise ratio of the AMS measurement is defined by counting statistics. Generally, the smaller the sample, the shorter the measurement time, the higher the uncertainty. For defining the contamination contribution of the overall instrument setup (constant contamination) and the memory effect between subsequent samples of very different ^{14}C content and carbon mass (cross contamination), a series with varying amounts of solid grains of fossil NaOAc and the modern reference material oxalic acid II was combusted with the Sunset and measured for its ^{14}C content. The constant contaminant mass was estimated as 0.4 ± 0.2 µg carbon with a $F^{14}C$ of 0.8 ± 0.4 and for the cross contamination $0.5 \pm 0.4\%$ of the carbon of the previous sample was found to mix with the next injection (Agrios et al., 2015).

The total carbon amounts in ice cores are rather low, in the µg/kg-range. Because of that, each step of sample preparation implies a potential risk of contamination with either modern or fossil carbon. Thus a large contribution to the final overall uncertainty on the age is induced by the procedural blank correction, especially for small size samples. It is therefore crucial that cutting, melting and filtrating the ice results in the lowest possible procedural blank with a stable $F^{14}C$ value to ensure a high and stable signal-to-blank ratio for obtaining reliable results with the smallest possible uncertainties. Procedural blanks were estimated using artificial ice blocks of frozen ultra-pure water, treated in the same way as real ice samples (Jenk et al., 2007). Blanks were usually prepared together with samples and their analysis was performed during every AMS measurement session (Sunset combustion and AMS analysis). The mean of the overall procedural blank (WIOC) used to correct all samples is 1.34 ± 0.62 µg of carbon with a $F^{14}C$ of 0.69 ± 0.13 (100 and 54 measurements, respectively, performed over a 10-year period). This includes all values obtained with both, the THEODORE and Sunset system. We decided to use this combined value, since the ice sample preparation step is the by far largest contribution to the blank and is system independend. This mean value is consistent with previously reported results (Jenk et al., 2007; Sigl et al., 2009), indicating the long-term stability of the procedural blanks.

In summary, all the corrections have the strongest effect on low carbon mass samples, resulting in the largest dating uncertainties. Further, such small samples can only be measured for a short period of time, with reduced stability of the ^{12}C current, additionally worsening of the signal-to-noise ratio. Low carbon mass samples of old age contain even a lower number of ^{14}C compared to younger samples due to radioactive decay and are affected the most. Among all uncertainties described, the correction for the procedural blank contributes typically around 60%. As an example, for hypothetical samples with a WIOC mass of 5 or 10 µg, the resulting uncertainty of the finally calibrated ages for 1000 year old ice would be around ± 600 yrs or ± 250 yrs and for 8000 year old ice around ± 1600 yrs or ± 700 yrs, respectively. Hence by doubling the mass, the uncertainty is reduced by more than 50%. We therefore generally discuss dating results only for sample masses larger than ~10 µg WIOC, which have an acceptable age uncertainty in the range of 10-20%.

While calibrating the ages with the OxCal, a sequence constraint can be applied based on the assumption of a monotonous increase of age with depth (Bronk Ramsey, 2008). This approach often leads to a reduction of the final uncertainty, which however strongly depends on the sample resolution with depth, see example in Jenk et al. (2009).

5 Validation of the dating accuracy

5.1. First attempts

Validating the accuracy of the here described approach for ^{14}C dating of ice is a challenging task since it requires ice samples
250 with known ages, preferentially covering a large age range. First attempts for validation by dating ice from Greenland with an age determined by annual layer counting failed, because WIOC concentrations are an order of magnitude lower compared to ice from glaciers located closer to biogenic emission sources (Figure 2). Large ice samples were thus needed, nevertheless resulting in small amounts of carbon. Our preparation method is not optimised for such sample sizes, and the required pooling of several pieces of ice may have induced a higher procedural blank. As a result ^{14}C ages tended to be biased by the
255 procedural blank value (Sigl et al., 2009). ^{14}C ages of the Fiescherhorn ice core (Jenk et al., 2006) ranged from modern values to 1000 years, thus reasonably matching the age of the ice older than AD 1800 obtained by annual layer counting. For the ice core from Mercedario (31.98° S, 70.13° W; 6100 m a.s.l.) the deepest core sections show ages of <550 and 320–1120 cal BP, respectively, well in line with a tentative chronology based on annual layer counting (Sigl et al., 2009). However, considering the relatively large uncertainty of our method if compared to conventional ^{14}C dating typically derived from
260 samples with much larger carbon masses and the flatness of the ^{14}C calibration curve between around 500 and 0 cal BP such samples of rather young ages are not ideal for a precise validation. Two samples from the Illimani ice core, bracketing the AD 1258 volcanic eruption time marker resulted in a combined calibrated age of AD 1050±70 (1 σ) overestimating the expected age by around 200years. This would be an acceptable accuracy if applicable to several thousand years old ice (Sigl et al. 2009).
265 Overall these were first indications that the ^{14}C method gives reliable ages. Meanwhile we have had access to independently dated ice from the Juvfonne ice patch and the Quelccaya ice cap, dated a fly which we discovered in the Tsambagarav ice core, and dated ice cores from Mt. Ortles glacier, in which a larch leaf was found, altogether allowing a more robust validation as outlined in the following.

5.2. Recent validation

270 Juvfonne is a small perennial ice patch in the Jotunheimen Mountains in central southern Norway (61.68° N, 8.35° E). In May 2010, a 30-m-long ice tunnel was excavated, revealing several up to 5 cm thick dark organic-rich layers containing organic remains , which were interpreted as previous ice-patch surfaces and conventionally ^{14}C dated (Nesje et al., 2012). We received two samples of clear ice adjacent to the organic-rich layers and a surface sample (JUV 1, JUV 2, JUV 3, Table 3). The results derived using WIOC agreed well with the corresponding, conventionally dated ^{14}C ages with an age range
275 between modern and 2900 cal BP (Zapf et al., 2013). In summer 2015 we collected additional clear ice samples adjacent to a conventionally ^{14}C dated plant fragment found in an organic-rich layer at the base of a new tunnel excavated in 2012 and extending deeper into the ice patch (Ødegård et al., 2016). Four ice blocks were collected and afterwards subdivided in two sub-samples each. Ice block 1 (JUV 0_1 and JUV 0_2) was taken adjacent to the plant fragment layer, ice block 2 (JUV 0_3 and JUV 0_4), ice block 3 (JUV 0_5 and JUV 0_6) and ice block 4 (JUV 0_7 and JUV 0_8) at the bottom of the wall, a few
280 cm below the plant fragment layer. JUV 0_1 and JUV 0_2 yielded an average age of 6988 ± 268 cal BP, which is in good agreement with the age of the plant fragment layer of 6609 ± 48 cal BP, considering the observed increase in ages with increasing depth. Accordingly, the other six samples collected even further below this organic-rich layer resulted in significantly older ages (7631 ± 155 cal BP, Table 3).

Three sections of the ice core from the Quelccaya Summit Dome drilled in 2003 (QSD, Peruvian Andes, 168.68 m, 13°56'S,
285 70°50'W, 5670 m a.s.l.) were kindly provided by Lonnie Thompson, Ohio State University. The entire ice core was dated by annual layer counting indicating an age of 1800 years at the bottom (Thompson et al., 2013). Intentionally we received the samples without knowing their ages or depths in order to have the opportunity to perform a "blind test". The three sections were not decontaminated as usual, but only rinsed with ultra-pure water, because the amount was not large enough for

removing the outer layer mechanically. As shown in Figure 3 (see also Table 4 for the results) the resulting calibrated ages agree very well with the ages based on annual layer counting (L. Thompson, personal communication 2015).

Recently a number of core segments of the previously dated Tsambagarav ice core (Herren et al., 2013) were resampled. In segment 102 a tiny insect (Figure 4) was found and immediately separated from the ice matrix. Since it was small, a conventional ^{14}C analysis was not suitable and instead the Sunset-AMS system was deployed. The ice section containing the fly was melted, possible contamination from carbonates and humic acids were removed by an acid-base-acid treatment at 40°C (Szidat et al., 2014), the fly was dried, placed onto a quartz fibre filter and combusted in the Sunset, resulting in 13 µg of carbon. The age of 3442 ± 191 cal BP (BE-5013.1.1) is in perfect agreement with the age of WIOC from this ice segment of 3495 ± 225 cal BP (Herren et al., 2013) (Figure 3).

Additionally, we dated three sections from a set of ice cores drilled in 2011 on Mt. Ortles (see Table 1 for location) for which a preliminary age of 2612 ± 101 cal BP was derived by conventional ^{14}C dating of a larch leaf found at 73.2 m depth (59.60 m weq, ~1.5 m above bedrock) (Gabrielli et al., 2016). Every section was horizontally divided in three sub-samples (top, middle, bottom). For the section at 68.61 m depth (55.08 m weq, core #1) and the section at 71.25 m depth (57.94 m weq, core #3), the ages obtained for the sub-samples were not significantly different from each other especially if accounting for the expected thinning of annual layer thickness at these depths (Figure 5). Accordingly the results of the respective sub-samples were combined to derive the most accurate ages for the mid-depths of these two sections (mean $F^{14}C$ with the estimated 1σ uncertainty being the standard error of the unbiased standard deviation).. On the contrary the ages of the three sub-samples from the deepest section at 74.13 m (60.54 m weq, core #3) significantly increased with depth, implying strong glacier thinning close to bedrock (see also Gabrielli et al., 2016 , this issue). Our WIOC ^{14}C ages obtained for the Mt. Ortles ice core agree well with the age of the larch leaf assuming an exponential increase of age with depth (Figure 5).

The scatter plot in Figure 3 summarizes the different validation experiments described above. The results for the Mt. Ortles ice core were not included because larch leaf and WIOC samples were extracted from depths of significantly different ages. As shown, within the uncertainties, the ^{14}C ages fall onto the 1:1 line in the age range from ~700-3500 cal BP, convincingly demonstrating good accuracy of our method. All validation experiments were performed on low-dust samples, thus avoiding potential dating bias due to the presence of dust (Hoffmann, 2016).

6 Applications and current potential of the ^{14}C method for dating glacier ice

Over the last 10 years the deepest parts of several ice cores have been dated applying the presented WIOC ^{14}C method. To illustrate the current potential of the method with respect to the time period accessible we compiled five ice core chronologies in Figure 6. The sites differ in recent net annual snow accumulation and ice thickness (in brackets): Tsambagarav ice cap in the Mongolian Altai 0.33 m weq (72 m) (Herren et al., 2013), Belukha glacier in the Siberian Altai 0.34 m weq (172 m) (Aizen et al., 2016), Colle Gnifetti glacier in the European Alps 0.46 m weq (80 m) (Jenk et al., 2009), Illimani glacier in the Bolivian Andes 0.58 m weq (138.7 m) (Kellerhals et al., 2010), Mt. Ortles glacier 0.85 m weq (75 m) (Gabrielli et al., 2016 , this issue). All of these are cold glaciers and frozen to the bedrock with the exception of Mt. Ortles glacier, which is polythermal and experienced a recent acceleration of glacier flow due to sustained atmospheric warming over the past decades (Gabrielli et al., 2016 , this issue). To derive a continuous age depth relationship, a two parameter flow model (Bolzan, 1985; Thompson et al., 1990) was applied for Colle Gniffetti (Jenk et al., 2009), Illimani (Kellerhals et at., 2010) and here also for the core from Belukka using the data presented in Aizen et al. (2016). A different approach as discussed below, was implemented for the ice cores from the Tsambagarav ice cap (Herren et al., 2013) and the glacier on Mt. Ortles (see also Gabrielli et al., 2016 , this issue). The two parameter model is based on a simple analytical expression for the decrease of the annual layer thickness $L_{(z)}$ (m weq) with depth:

$$L_{(z)} = b(1 - \frac{z}{H})^{p+1}$$

where z is depth (m weq), H the glacier thickness (m weq), b the annual accumulation (m weq) and p a thinning parameter
330 (dimensionless). The age T(z) as a function of depth can be calculated when the inverse layer thickness is integrated over depth:

$$T_{(z)} = \int \frac{dz}{L_{(z)}} = \frac{1}{b} \int (1 - \frac{z}{H})^{-p-1} dz$$

Solving the integral and setting the age at the surface to be T(0) = 0, the final age-depth relation is obtained:

$$T_{(z)} = \frac{H}{bp}[(1 - \frac{z}{H})^{-p} - 1]$$

The thinning rate (vertical strain rate) is the first derivative of the layer thickness:

$$L'_{(z)} = \frac{dL_{(z)}}{dz} = -\frac{b(p+1)}{H}(1 - \frac{z}{H})^p$$

The model has two degrees of freedom, the net annual accumulation rate b and the thinning parameter p both assumed to be
335 constant over time. This allows to fit the model by a least squares approach through the available reference horizons if the glacier thickness H is known (if drilled to bedrock) or can be reasonably well estimated (e.g. from radar sounding). In order to not overweight the data from the deepest horizons, the model is fitted using the logarithms of the age values. For the ice cores from Colle Gnifetti (Jenk et al., 2009), Illimani (Kellerhals et al., 2010) and Belukha (Aizen et al., 2016) these ages were based on annual layer counting, identification of reference horizons (radioactive fallout and well-known volcanic
340 eruptions) and ^{14}C dates. The data is summarized in Table 1. In Figure 6, only reference horizons and ^{14}C dates were included for simplification.

In summary, a reasonable fit was achieved for these three glaciers and the derived annual net accumulations (Colle Gnifetti 0.45±0.03 m weq, Belukha 0.36 ± 0.03 m weq, Illimani 0.57 ± 0.13 m weq) are comparable with the values previously published (see above), which were determined either by surface measurements or were estimated based on ALC or/and the
345 uppermost age horizons only (e.g. nuclear fallout peak), thereby accounting for the (slight) layer thinning occuring in these uppermost few meters (Nye, 1963). Since the assumption of constant accumulation (b) and a constant thinning parameter (p) over time/with depth is likely only true in a first order approximation it is thus no surprise thatthe two parameter model mayfail to result in a reasonable fit within the derived age uncertainties. In such a case these two underlying assumptions should then be investigated more thoroughly as it was e.g. donefor the ice cores from Tsambagarav and Mt. Ortles. Whereas
350 Tsambagarav also is a cold glacier, Mt. Ortles is polythermal. For Tsambagarav, a good fit can be achieved if additional degree of freedom is given to account for variations in the net accumulation rate while p is fixed to the initially derived value, suggesting significant changes in the accumulation rate over time. This is supported by the fact that the resulting strong variation in net accumulation is consistent with precipitation changes in the Altai derived from lake sediment studies (Herren et al., 2013). Opposite to that, a reasonable fit for the Mt. Ortles ice core can only be obtained if the thinning
355 parameter p is allowed to increase with depth, while the annual net accumulation is assumed to be constant over time (i.e. b fixed to the value defined by the stake measurements and surface layers). This points to an exceptionally strong thinning. Mt. Ortles glacier is polythermal with temperate conditions in the upper part and still relatively warm ice with -2.8°C near bedrock. We hypothesize that the faster horizontal velocity of the warm ice causes exceptional horizontal stress (internal horizontal deformation) on the ice frozen to the bedrock, resulting in stronger thinning. In both cases, a purely empirical
360 approach of fitting the age horizons was chosen to establish the age-depth relationship. Note that due to the lack of absolute time markers prior to 1958, ^{210}Pb dated horizons were used for Mt. Ortles . For Tsambagarav a combination of different polynomial functions was used (Herren et al., 2013), whereas a slightly more sophisticated approach by means of Monte Carlo simulation was applied for Mt. Ortles, allowing an objective uncertainty estimate for each depth defined by the density of dating horizons and their individual uncertainty (Gabrielli et al., 2016 , this issue). These purely empirical approaches are
365 justified given the high confidence assigned to the determined ages for the dated horizons.

As shown in Figure 6, the time period dated with ^{14}C ranges from 200 to more than 10000 yrs. Due to their uncertainty, ^{14}C ages derived by our method cannot compete with the conventional methods for dating ice that is only a few centuries old. The strength of ^{14}C dating using WIOC is that it allows obtaining absolute ages from basically every piece of ice from cold and polythermal ice bodies. This is especially valuable for glaciers not containing the last glacial/interglacial transition, as Tsambagarav and Mt. Ortles, since in such cases not even climate wiggle matching of the transition signal with other dated archives is possible. Anyhow, an absolute dating method is preferable to wiggle matching, which is not necessarily reliable. For example, a depletion in $\delta^{18}O$ presumably indicating the LGM-Holocene transition might not always be a true atmospheric signal, but can be caused by unknown mechanisms potentially happening close to bedrock (Jenk et al., 2009; Wagenbach et al., 2012). All five examples show strong thinning towards bedrock with the oldest ages obtained being in the range of 10000 years. Because of the strong thinning, the ^{14}C age of the deepest sample represents a strongly mixed age of ice with a large age distribution. In these cases, the age limit was thus not determined by the ^{14}C half-life of 5730 yrs (Godwin, 1962), but by the achievable spatial depth resolution since some hundred grams of ice is required. .

Since an absolute WIOC mass of ~10 µg is needed to achieve a ^{14}C dating with reasonably low uncertainty, the overall applicability of the method essentially depends on the WIOC concentration in the ice and the ice mass available. Figure 2 summarizes WIOC concentrations determined in ice from various locations around the globe. In general, mid-latitude and low-latitude glaciers contain sufficient WIOC from 21 to 295 µg/kg, allowing dating with less than 1 kg of ice. The highest concentration was found at Juvfonne ice patch which is small and located a low elevation and therefore by far closest to biogenic emission sources. WIOC concentrations might be further elevated due to meltwater and superimposed ice formation, enriching water-insoluble particles in the surface layer present at that time. Lowest concentrations of only 2 to 15 µg/kg WIOC were observed in polar snow and ice from Greenland and Antarctica. For this concentration range a reliable dating is impossible with the current method capability.

7 Conclusions

Since the introduction about 10 years ago of the ^{14}C dating technique for glacier ice, utilizing the WIOC fraction of carbonaceous aerosol particles embedded in the ice matrix, major improvements in separating the OC from the EC fraction and in AMS technology have been achieved. The new configuration with direct coupling of a commercial thermo-optical OC/EC analyser to the gas ion source of the MICADAS AMS via its gas introduction interface has two major advantages. First, the measurement time was significantly reduced to approximately 35 min per sample. Second, the implemented automated protocol allows for a controlled routine analysis with high reproducibility and a stable blank, thereby increasing the overall precision.

The presented WIOC ^{14}C dating method was validated by determining the age of independently dated ice samples. It principally allows absolute and accurate dating of any piece of ice containing sufficient WIOC. With the current setup, the age of samples with a minimum of ~10 µg WIOC can be determined with satisfying precision of about 10 to 20%, depending on the age. This requires about 300 to 800 g of ice,considering both, the mass loss of 20-30% during surface decontamination and the WIOC concentrations typically found in mid- and low latitude glaciers. Dating polar ice with satisfactory age uncertainties is still not possible since WIOC concentrations are around one order of magnitude lower. This would require further reduction of the procedural blank for such samples requiring larger ice volumes which potentially could be achieved by an additional, specifically designed sample preparation setup for such kind of samples.

The ^{14}C method is suitable for dating ice with ages from 200 to more than 10000 yrs. Whereas for a few century old ice the conventional dating methods are typically higher in precision, the WIOC ^{14}C method presents the only option for obtaining reliable continuous time scales for the older and deeper ice core sections of mountain glaciers. This is not only crucial for interpreting the embedded environmental and climatic history, but gives additional insight into glacier flow dynamics close

to bedrock as demonstrated by the depth-age scales derived from ^{14}C dating of ice cores from various mid- and low latitude glaciers. Also, it can reveal information about the time of glacier formation.

Acknowledgements

410   This work was supported by the Swiss National Science Foundation (200020_144388) and by the Oeschger Centre for Climate Change Research of the University of Bern. We thank Sandra Brügger and Edith Vogel for sample preparation of the fly extracted from the Tsambagarav ice core.

Author contribution

Manuscript written by C.U., T.M.J. and M.Sch. with editing by S.S. Sample preparation and ^{14}C measurements performed by
415   C.U., A.Z. and M.S. with expert supervision of G.S., S.S.. and T.M.J..

References

Agrios, K., Salazar, G., Zhang, J.-L., Uglietti, C., Battaglia, M., Luginbühl, M., Ciobanu, V. G., Vonwiller, M., and Szidat, S.: Online coupling of pure O$_2$ thermo-optical methods – ^{14}C AMS for source apportionment of carbonaceous aerosols, Nuclear Instruments and Methods in Physics Research B, 361, 288-293, 2015.

420   Aizen, E. M., Aizen, V. B., Takeuchi, N., Joswiak, D. R., Fujita, K., Nikitin, S. A., Grigholm, B., Zapf, A., Mayewski, P., Schwikowski, M., and Nakawo, M.: Abrupt and moderate climate changes in the mid-latitudes of Asia during the Holocene, Journal of Glaciology, 62, 233, 411-439, 2016.

Bolzan, J. F.: Ice Flow at the Dome-C Ice Divide Based on a Deep Temperature Profile, Journal of Geophysical Research-Atmospheres, 90, (D5), 8111–8124, 1985.

425   Bronk Ramsey, C.: Deposition models for chronological records, Quaternary Science Reviews, 27, 1-2, 42–60, 2008.

Bronk Ramsey, C. and Lee, S.: Recent and planned developments of the program Oxcal, Radiocarbon, 55, 2-3, 720–730, 2013.

Cao, F., Zhang, J. L., Szidat, S., Zapf, A., Wacker, L., and Schwikowski, M.: Microgram-level radiocarbon determination of carbonaceous particles in firn and ice samples: pretreatment and OC/EC separation, Radiocarbon, Vol 55, No. 2-3, 2013.

430   Drosg, R., Kutschera, W., Scholz, K., Steier, P., Wagenbach, D., and Wild, E. M.: Treatment of small samples of particulate organic carbon (POC) for radiocarbon dating of ice, Nuclear Instruments and Methods in Physics Research Section B: Beam Interactions with Materials and Atoms, 259, No. 1, 340-344, doi: 10.1016/j.nimb.2007.02.094, 2007.

Eichler, A., Olivier, S., Henderson, K., Laube, A., Beer, J., Papina, T., Gäggeler, H. W., and Schwikowski, M.: Temperature response in the Altai region lags solar forcing, Geophys Res Lett, 36, L01808, doi:10.1029/2008GL035930, 2009.

435   Eichler, A., Schwikowski, M., Gäggeler, H. W., Furrer, V., Synal, H.-A., Beer, J., Saurer, M., and Funk, M.: Glaciochemical dating of an ice core from upper Grenzgletscher (4200ma.s.l.), Journal of Glaciology, 46, 507–515, 2000.

Gabrielli, P., Barbante, C., Bertagna, G., Bertó, M., Binder, D., Carton, A., Carturan, L., Cazorzi, F., Cozzi, G., Dalla Fontana, G., Davis, M., De Blasi, F., Dinale, R., Dragà, G., Dreossi, G., Festi, D., Frezzotti, M., Gabrieli, J., Galos, S. P., Ginot, P., Heidenwolf, P., Jenk, T., Kehrwald, N., Kenny, D., Magand, O., Mair, V., Mikhalenko, V., Lin, P. N., Oeggl, K.,
440   Piffer, G., Rinaldi, M., Schotterer, U., Schwikowski, M., Seppi, R., Spolaor, A., Stenni, B., Tonidandel, D., Uglietti, C., Zagorodnov, V. S., Zanoner, T., and Zennaro, P.: Age of the Mt. Ortles ice cores, the Tyrolean Iceman and glaciation of the highest summit of South Tyrol since the Northern Hemisphere Climatic Optimum, The Cryospheredoi:10.5194/tc-2016-159, special issue for IPICS, doi:10.5194/tc-2016-159, 2016

Gäggeler, H. W., Von Gunten, H. R., Rössler, E., Oeschger, H., and Schotterer, U.: ^{210}Pb-dating of cold alpine firn/ice cores
445   from Colle Gnifetti, Switzerland, Journal of Glaciololgy, 29, No. 101, 165– 177, 1983.

Gavin, D. G.: Estimation of inbuilt age in radiocarbon ages of soil charcoal for fire history studies, RADIOCARBON, 43, 1, 27–44 2001.

Gelencsér, A.: Major Carbonaceous particle types and their sources., In: Carbonaceous Aerosol. Springer, The Netherlands, 45–147, 2004.

Gelencsér, A., May, B., Simpson, D., Sánchez-Ochoa, A., Kasper-Giebl, A., Puxbaum, H., Caseiro, A., Pio, C., and Legrand, M.: Source apportionment of PM2.5 organic aerosol over Europe: Primary/secondary, natural/anthropogenic, and fossil/biogenic origin, Journal of Geophysical Research, 112, D23S04, doi: 10.1029/2006JD008094, 2007.

Godwin, H.: Half-life of Radiocarbon., Nature, 195, 4845, 1962.

Hallquist, M., Wenger, J. C., Baltensperger, U., Rudich, Y., Simpson, D., Claeys, M., Dommen, J., Donahue, N. M., George, C., Goldstein, A. H., Hamilton, J. F., Herrmann, H., Hoffmann, T., Iinuma, Y., Jang, M., Jenkin, M. E., Jimenez, J. L., Kiendler-Scharr, A., Maenhaut, W., McFiggans, G., Mentel, T. F., Monod, A., Prévot, A. S. H., Seinfeld, J. H., Surratt, J. D., Szmigielski, R., and Wildt, J.: The formation, properties and impact of secondary organic aerosol: current and emerging issues, Atmos. Chem. Phys., 9, 5155–5236, 2009.

Herren, P. A., Eichler, A., Machguth, H., Papina, T., Tobler, L., Zapf, A., and Schwikowski, M.: The onset of Neoglaciation 6000 years ago in western Mongolia revealed by an ice core from the Tsambagarav mountain range, Quaternary Science Reviews, 69, 59-68, doi: 10.1016/j.quascirev.2013.02.025, 2013.

Hoffmann, H. M.: Micro radiocarbon dating of the particulate organic carbon fraction in Alpine glacier ice: method refinement, critical evaluation and dating applications, Phd Thesis, Doctor of Natural Sciences, Natural Sciences and Mathematics, Ruperto-Carola University of Heidelberg, Germany, 2016.

Hogg, A. G., Hua, Q., Blackwell, P. G., Niu, M., Buck, C. E., Guilderson, T. P., Heaton, T. J., Palmer, J. G., Reimer, P. J., Reimer, R. W., Turney, C. S. M., and Zimmerman, S. R. H.: ShCal13 Southern Hemisphere Calibration, 0-50,000 Years Cal BP, Radiocarbon, 55, No. 4, 1889-1903, 2013.

Jenk, T. M., Szidat, S., Bolius, D., Sigl, M., Gäggeler, H. W., Wacker, L., Ruff, M., Barbante, C., Boutron, C. F., and Schwikowski, M.: A novel radiocarbon dating technique applied to an ice core from the Alps indicating late Pleistocene ages, Journal of Geophysical Research, 114, D14305, doi: 10.1029/2009jd011860, 2009.

Jenk, T. M., Szidat, S., Schwikowski, M., Gäggeler, H. W., Brütsch, S., Wacker, L., Synal, H. A., and Saurer, M.: Radiocarbon analysis in an Alpine ice core: record of anthropogenic and biogenic contributions to carbonaceous aerosols in the past (1650–1940), Atmos Chem Phys, 6, 5381–5390, 2006.

Jenk, T. M., Szidat, S., Schwikowski, M., Gäggeler, H. W., Wacker, L., Synal, H. A., and Saurer, M.: Microgram level radiocarbon (^{14}C) determination on carbonaceous particles in ice, Nuclear Instruments and Methods in Physics Research Section B: Beam Interactions with Materials and Atoms, 259, No. 1, 518-525, doi: 10.1016/j.nimb.2007.01.196, 2007.

Kaspari, S., Schwikowski, M., Gysel, M., Flanner, M. G., Kang, S., Hou, S., and Mayewski, P. A.: Recent increase in black carbon concentrations from a Mt. Everest ice core spanning 1860-2000 AD, Geophys Res Lett, 38, L04703, doi: 10.1029/2010gl046096, 2011.

Kellerhals, T., Brütsch, S., Sigl, M., Knüsel, S., Gäggeler, H. W., and Schwikowski, M.: Ammonium concentration in ice cores: A new proxy for regional temperature reconstruction?, Journal of Geophysical Research: Atmospheres, 115, D16, 2156-2202, 2010.

Lavanchy, V. M. H., Gäggeler, H. W., Schotterer, U., Schwikowski, M., and Baltensperger, U.: Historical record of carbonaceous particle concentrations from a European high-alpine glacier (Colle Gnifetti, Switzerland), Journal of Geophysical Research, 104, D17, 21'227 - 221'236, doi:10.1029/1999JD900408., 1999.

Legrand, M., Preunkert, S., Jourdain, B., Guilhermet, J., Faïn, X., Alekhina, I., and Petit, J. R.: Water-soluble organic carbon in snow and ice deposited at Alpine, Greenland, and Antarctic sites: a critical review of available data and their atmospheric relevance, Climate of the Past, 9, 2195–2211, 2013.

Legrand, M. and Puxbaum, H.: Summary of the CARBOSOL project: Present and retrospective state of organic versus inorganic aerosol over Europe, Journal of Geophysical Research, 112, D23S01, doi:10.1029/2006JD008271, 2007.

Lüthi, M. P. and Funk, M.: Modelling heat flow in a cold, high altitude glacier: interpretation of measurements from Colle Gnifetti, Swiss Alps., Journal of Glaciology, 47, No. 157, 314-324, 2001.

May, B., Wagenbach, D., Hoffmann, H., Legrand, M., Preunkert, S., and Steier, P.: Constraints on the major sources of dissolved organic carbon in Alpine ice cores from radiocarbon analysis over the bomb-peak period, Journal of Geophysical Research: Atmospheres, 118, 3319–3327, 2013.

McConnell, J. R., Aristarain, A. J., Banta, J. R., Edwards, P. R., and Simoes, J. C.: 20th-Century doubling in dust archived in an Antarctic Peninsula ice core parallels climate change and desertification in South America, Proceedings of the National Academy of Sciences of the United States of America 104, No. 14, 5743-5748, 10.1073/pnas.0607657104, 2007.

Mook, W. G. and van der Plicht, J.: Reporting ^{14}C activities and concentrations, Radiocarbon, 41, No. 3, 1999.

Moore, J. C., Beaudon, E., Kang, S., Divine, D., Isaksson, E., Pohjola, V. A., and van de Wal, R. S. W.: Statistical extraction of volcanic sulphate from nonpolar ice cores, Journal of Geophysical Research: Atmospheres, 117, pp. D03306/1 - D03306/16, 2012.

Nesje, A., Pilo, L. H., Finstad, E., Solli, B., Wangen, V., Odegard, R. S., Isaksen, K., Storen, E. N., Bakke, D. I., and Andreassen, L. M.: The climatic significance of artefacts related to prehistoric reindeer hunting exposed at melting ice patches in southern Norway., The Holocene, 22, No. 4, 485–496, 2012.

Nye, J. F.: Correction factor for accumulation measured by the thickness of the annual layers in an ice sheet, journal of Glaciology, 4, 785–788, 1963.

Ødegård, R. S., Nesje, A., Isaksen, K., Andreassen, L. M., Eiken, T., Schwikowski, M., and Uglietti, C.: Climate change threatens archeologically significant ice patches: insights into their age, internal structure, mass balance and climate sensitivity, The Cryospheredoi:10.5194/tc-2016-94, doi:10.5194/tc-2016-94, 2016.

Preunkert, S., D., W., Legrand, M., and Vincent, C.: Col du Dome (Mt Blanc Massif, French Alps) suitability for ice-core studies in relation with past atmospheric chemistry over Europe., Tellus Series B-Chemical and physical meteorology, 52, 3, 993-1012, 2000.

Reimer, P. J., Bard, E., Bayliss, A., Beck, J. W., Blackwell, P. G., Ramsey, C. B., Buck, C. E., Cheng, H., Lawrence Edwards, R., Friedrich, M., Grootes, P. M., Guilderson, T. P., Haflidason, H., Irka Hajdas, I., Hatté, C., Heaton, T. J., Hoffmann, D. L., Hogg, A. G., Hughen, K. A., Kaiser, K. F., Kromer, B., Manning, S. W., Niu, M., Reimer, R. W., Richards, D. A., Scott, E. M., Southon, J. R., Staff, R. A., Turney, C. S. M., and van der Plicht, J.: IntCal13 and marine13 radiocarbon age calibration curve 0–50,000 years cal BP, RADIOCARBON, 55, 4, 1869–1887, 2013.

Ruff, M., S Fahrni, S., Gäggeler, H. W., Hajdas, I., Suter, M., Synal, H.-A., Szidat, S., and Wacker, L.: On-line radiocarbon measurements of small samples using elemental analyzer and MICADAS gas ion source., Radiocarbon, 52, No. 4, 1645–1656, 2010.

Ruff, M., Wacker, L., Gäggeler, H. W., Suter, M., Synal, H. A., and Szidat, S.: A gas ion source for radiocarbon measurements at 200 kV, Radiocarbon, 49, No. 2, 307-314, 2007.

Schwikowski, M.: Reconstruction of European air pollution from Alpine ice cores, in Earth Paleoenvironments: Records preserved in Mid- and Low-Latitude Glaciers, edited by L. D. Cecil, Green, J.R. and L. G. Thompson, 95-119, 2004.

Sigl, M., Jenk, T. M., Kellerhals, T., Szidat, S., Gäggeler, H. W., Wacker, L., Synal, H. A., Boutron, C. F., Barbante, C., Gabrieli, J., and Schwikowski, M.: Instruments and Methods Towards radiocarbon dating of ice cores, Journal of Glaciology, 55, No. 194, 985-996, 2009.

Steier, P., Drosg, R., Fedi, M., Kutschera, W., Schock, M., Wagenbach, D., and Wild, E. M.: Radiocarbon determination of particulate organic carbon in non-temperated, alpine glacier ice, Radiocarbon, 48, No. 1, 69–82, 2006.

Stuiver, M. and Polach, H. A.: Reporting of C-14 data – discussion, Radiocarbon, 19, 355-363, 1977.

Synal, H. A., Jacob, S., and Suter, M.: The PSI/ETH small radiocarbon dating system, Nuclear Instruments and Methods in Physics Research B, 172, 1-7, 2000.

Synal, H. A., Stocker, M., and Suter, M.: MICADAS: A new compact radiocarbon AMS system, Nuclear Instruments and Methods in Physics Research Section B: Beam Interactions with Materials and Atoms, 259, No. 1, 7-13, 10.1016/j.nimb.2007.01.138, 2007.

Szidat, S., Jenk, T. M., Gäggeler, H. W., Synal, H. A., Fisseha, R., Baltensperger, U., Kalberer, M., Samburova, V., Wacker, L., Saurer, M., Schwikowski, M., and Hajdas, I.: Source apportionment of aerosols by ^{14}C measurements in different carbonaceous particle fractions, Radiocarbon, 46, No. 1, 475-484, 2004a.

540 Szidat, S., Jenk, T. M., Gäggeler, H. W., Synal, H. A., Hajdas, I., Bonani, G., and Saurer, M.: THEODORE, a two-step heating system for the EC/OC determination of radiocarbon (^{14}C) in the environment, Nuclear Instruments and Methods in Physics Research Section B: Beam Interactions with Materials and Atoms, 223-224, 829-836, 10.1016/j.nimb.2004.04.153, 2004b.

Szidat, S., Salazar, G. A., Battaglia, M., Wacker, L., Synal, H.-A., Vogel, E., and Türler, A.: ^{14}C analyses and sample
545 preparation at the new Bern Laboratory for the Analyses of Radiocarbon with AMS (LARA), Radiocarbon, 56, No. 2, 561–566, 2014.

Thompson, L. G., Davis, M. E., Mosley-Thompson, E., Sowers, T. A., Henderson, K. A., Zagorodnov, V. S., Lin, P. N., Mikhalenko, V. N., Campen, R. K., Bolzan, J. F., Cole-Dai, J., and Francou, B.: A 25,000-Year Tropical Climate History from Bolivian Ice Cores, Science, 282, No. 5395, 1858-1864, 10.1126/science.282.5395.1858, 1998.

550 Thompson, L. G., Mosley-Thompson, E., Davis, M., Bolzan, J. F., Dai, J., Klein, L., Gundestrup, N., Yao, T., Wu, X., and Xie, Z.: Glacial stage ice-core records from the subtropical Dunde ice cap, China, Annals of Glaciology, 14, 288-297, 1990.

Thompson, L. G., Mosley-Thompson, E., Davis, M., Henderson, K., Brecher, H. H., Zagorodnov, V. S., Mashiotta, T. A., Lin, P. N., Mikhalenko, V. N., Hardy, D. R., and Beer, J.: Kilimanjaro ice core records: Evidence of Holocene climate change in Tropical Africa, Science, 298, No. 5593, 589-593, 2002.

555 Thompson, L. G., Mosley-Thompson, E., Davis, M. E., Zagorodnov, V. S., Howat, I. M., Mikhalenko, V. N., and Lin, P. N.: Annually Resolved Ice Core Records of Tropical Climate Variability over the Past ~1800 Years, Science, 340, 6135, 945-950, 2013.

Wacker, L., Bonani, G., Friedrich, M., Hajdas, I., Kromer, B., Němec, M., Ruff, M., Suter, M., Synal, H. A., and Vockenhuber, C.: MICADAS: routine and high-precision radiocarbon dating, Radiocarbon, 52, No. 2-3, 252-262, 2010.

560 Wagenbach, D., Bohleber, P., and Preunkert, S.: Cold alpine ice bodies revisited: what may we learn from their impurity and isotope content? , Geogr. Ann: Series A, Physical Geography, 94, 245–263, 10.1111/j.1468-0459.2012.00461.x, 2012.

Zapf, A., Nesje, A., Szidat, S., Wacker, L., and Schwikowski, M.: ^{14}C measurements of ice samples from the Juvfonne ice tunnel, Jotunheimen, Southern Norway—validation of a ^{14}C dating technique for glacier ice, Radiocarbon, 55, No. 2–3, 571–578, 2013.

565 Zhang, Y.-L., Li, J., Zhang, G., Zotter, P., Huang, R.-J., Tang, J.-H., Wacker, L., Prévôt, A. S. H., and Szidat, S.: Radiocarbon-Based Source Apportionment of Carbonaceous Aerosols at a Regional Background Site on Hainan Island, South China, Environmental Science & Technology, 48, 2651–2659, 2014.

Zhang, Y.-L., Perron, N., Ciobanu, V. G., Zotter, P., Minguillón, M. C., Wacker, L., Prévôt, A. S. H., Baltensperger, U., and Szidat, S.: On the isolation of OC and EC and the optimal strategy of radiocarbon-based source apportionment of
570 carbonaceous aerosols, Atmos Chem Phys, 12, No. 22, 10841-10856, 10.5194/acp-12-10841-2012, 2012.

Zhang, Y.-L., Zotter, P., Perron, N., Prévôt, A. S. H., Wacker, L., and Szidat, S.: Fossil and non-fossil sources of different carbonaceous fractions in fine and coarse particles by radiocarbon measurement, Radiocarbon, 55, 3-4, 1510-1520, 2013.

Zotter, P., Ciobanu, V. G., Zhang, Y. L., El-Haddad, I., Macchia, M., Daellenbach, R., Salazar, G. A., Huang, R.-J., Wacker, L., Hueglin, C., Piazzalunga, A., Fermo, P., Schwikowski, M., Baltensperger, U., Szidat, S., and Prévôt, A. S. H.:
575 Radiocarbon analysis of elemental and organic carbon in Switzerland during winter-smog episodes from 2008 to 2012 – Part 1: Source apportionment and spatial variability, Atmos Chem Phys, 14, 13551–13570, 2014.

580 **Table 1:** Characteristics of the sites discussed and the respective dating approach. ALC stands for Annual Layer Counting, RH for Reference Horizons and ^{210}Pb, ^{3}H, and ^{14}C for nuclear dating. 2p model (two parameter model), MC (Monte Carlo simulation) and EF (exponential fit) denotes the applied approach to finally derive a continuous age-depth relationship (see Section 6 for details).

Site	Coordinates Elevation	Location	Dating approach	Time span (years)	References
Belukha	49.80°N, 86.55°E 4115 m a.s.l.	Altai Mountains, Russia	ALC, RH, ^{3}H, ^{14}C, 2p model	~9100	Aizen et al., 2016
Colle Gnifetti	45.93°N, 7.88°E 4450 m a.s.l.	Western Alps, Swiss-Italian border	ALC, RH, ^{3}H, ^{210}Pb, ^{14}C, 2p model	>15200	Jenk et al., 2009
Juvfonne	61.68°N, 8.35E 1916 m a.s.l.	Jotunheimen Mountains, Norway	^{14}C of plant fragment and WIOC	~7600	Zapf et al 2013 Ødegård et al., 2016
Illimani	17.03°S, 68.28°W 6300 m a.s.l.	Andes, Bolivia	ALC, RH, ^{3}H, ^{210}Pb, ^{14}C, 2p model	~12700	Sigl et al., 2009 Kellerhals et al., 2010
Mt. Ortles	46.51°N, 10.54°E 3905 m a.s.l.	Eastern Alps, Italy	ALC, RH, ^{3}H, ^{210}Pb, ^{14}C, MC	~6900	Gabrielli et al., 2016
Quelccaya	13.93°S, 70.83°W 5670 m a.s.l.	Andes, Peru	ALC, ^{14}C	~1800	Thompson et al., 2013
Tsambagarav	48.66°N, 90.86°E 4130 m a.s.l.	Altai Mountains, Mongolia	ALC, RH, ^{3}H, ^{210}Pb, ^{14}C, EF	~6100	Herren et al., 2013

585

Table 2: Samples analysed for the compararability test for OC/EC separation using the THEODORE apparatus and the Sunset OC/EC analyzer directly coupled to the AMS, with WIOC masses and concentrations. Calibrated ages (cal BP) denotes the 1 σ range.

590

Sample ID	AMS Lab. No.	WIOC mass (µg)	WIOC concentration µg/kg ice	$F^{14}C$	^{14}C age (BP)	cal age (cal BP)
1_THEODORE (JUV 3)	ETH 42845.1.1 ETH 42847.1.1 ETH 42849.1.1 ETH 43446.1.1	44	176	1.134 ± 0.017	-1010 ± 120	-46 - -7
1_Sunset (JUV 3)	BE 3683.1.1 BE 3701.1.1	46	119	1.157 ± 0.014	-1171 ± 97	-42 - -8
2_THEODORE (JUV 1)	ETH 43555.1.1 ETH 43557.1.1	18	60	0.743 ± 0.029	2386 ± 314	2011 - 2783
2_Sunset (JUV 1)	BE 3679.1.1	9	33	0.744 ± 0.021	2376 ± 225	2158 - 2737
3_THEODORE (BEL 1)	ETH 42841.1.1	18	63	0.771 ± 0.017	2089 ± 177	1886 - 2310
3_Sunset (BEL 1)	BE 4282.1.1	15	61	0.725 ± 0.022	2587 ± 233	2353 - 2924
4_THEODORE (BEL 2)	ETH 43448.1.1	15	47	0.402 ± 0.022	7320 ± 440	7686 - 8588
4_Sunset (BEL 2)	BE 4175.1.1	18	48	0.387 ± 0.022	7626 ± 457	7999 - 9011

Table 3: Juvfonne samples analysed for method validation. JUV 1, JUV 2 and JUV 3 were ice blocks collected from the 2010 tunnel (Zapf et al., 2013; Ødegård et al., 2016) and JUV 0 from the 2012 tunnel (Ødegård et al., 2016). To visualize the expected increase in age with increasing depth of the ice patch, samples are listed in stratigraphic order from top to bottom. Sample JUV 1 was collected between two separated organic-rich layers (Poz-56952 and Poz-36460). For comparision, an age range between these two layers was calculated (*, range between the lower and upper 2σ boundary, respectively). The results from sub-samples of the individual ice blocks were averaged to derive the combined values shown. Uncertainties (1σ) were calculated by error propagation of all analytical uncertainties for the individual measurements and for the combined values denote the standard error of the unbiased standard deviation. For a graphic display of the comparision see Fig. 3.

Sample ID	AMS Lab. No.	WIOC (µg)	g of ice	$F^{14}C$	^{14}C age (BP)	cal age (cal BP)
JUV 3_1	ETH 42845.1.1	55	292	1.124 ± 0.013	-939 ± 93	
JUV 3_2	ETH 42847.1.1	43	268	1.094 ± 0.015	-722 ± 110	
JUV 3_3	ETH 42849.1.1	47	325	1.155 ± 0.015	-1158 ± 104	
JUV 3_4	ETH 43446.1.1	43	208	1.164 ± 0.017	-1220 ± 117	
JUV 3 (surface 2010)				1.134 ± 0.017	-1010 ± 120	modern
Organic remains, Poz-37877				0.873 ± 0.003	1091 ± 28	963 - 1052
JUV 2_1	ETH 43443.1.1	27	215	0.881 ± 0.023	1018 ± 210	
JUV 2_2	ETH 43445.1.1	9	171	0.792 ± 0.066	1873 ± 669	
JUV 2_3	ETH 43559.1.1	17	257	0.870 ± 0.035	1119 ± 323	
JUV 2_4	ETH 45109.1.1	19	219	0.869 ± 0.031	1128 ± 287	
JUV 2 (2010)				0.853 ± 0.022	1277 ± 207	965 - 1368
Organic remains, Poz-56952*				0.777 ± 0.003	2027 ± 31	1929 - 2033
JUV 1_3	ETH 43555.1.1	20	281	0.766 ± 0.029	2141 ± 304	
JUV 1_4	ETH 43557.1.1	9	214	0.719 ± 0.064	2650 ± 715	
Organic remains, Poz-36460*				0.692 ± 0.003	2958 ± 35	3065 - 3174
JUV 1 (2010)				0.743 ± 0.029	2386 ± 314	2011 - 2783
Organic remains , age range between the two layers*				0.735 ± 0.037	2473 ± 404	2005 - 3004
Organic remains (plant fragment), Poz-56955				0.486 ± 0.002	5796 ± 33	6561 - 6656
JUV 0_1	BE 4184.1.1	393	283	0.479 ± 0.015	5913 ± 252	
JUV 0_2	BE 4380.1.1	246	298	0.457 ± 0.008	6290 ± 141	
JUV 0-A (2015)				0.468 ± 0.014	6099 ± 240	6720 - 7256
JUV 0_3	BE 4185.1.1	219	208	0.445 ± 0.012	6504 ± 217	
JUV 0_4	BE 4381.1.1	182	188	0.442 ± 0.007	6559 ± 127	
JUV 0_5	BE 4186.1.1	238	227	0.403 ± 0.012	7301 ± 239	
JUV 0_6	BE 4382.1.1	36	184	0.438 ± 0.011	6632 ± 202	
JUV 0_7	BE 4187.1.1	262	200	0.404 ± 0.011	7281 ± 219	
JUV 0_8	BE 4383.1.1	203	214	0.451 ± 0.013	6397 ± 232	
JUV 0-B (2015)				0.431 ± 0.009	6761 ± 168	7476 - 7785

Table 4: Quelccaya samples analysed for method validation. Calibrated ages (cal BP) denote the 1 σ range. ALC stands for Annual Layer Counting.

Sample	Depth (m)	AMS Lab. No.	WIOC (µg)	$F^{14}C$	^{14}C age (BP)	cal age (cal BP)	ALC (yrs BP)
139-140	144.69-146.79	BE 4336.1.1	15	0.888 ± 0.026	954 ± 237	675 - 1036	730 - 788
149-150	155.21-157.31	BE 4335.1.1	24	0.859 ± 0.018	1216 ± 171	1005 - 1300	1072 - 1157
157-158	163.88-166.09	BE 4337.1.1	14	0.803 ± 0.025	1761 ± 246	1414 - 1957	1439 - 1543
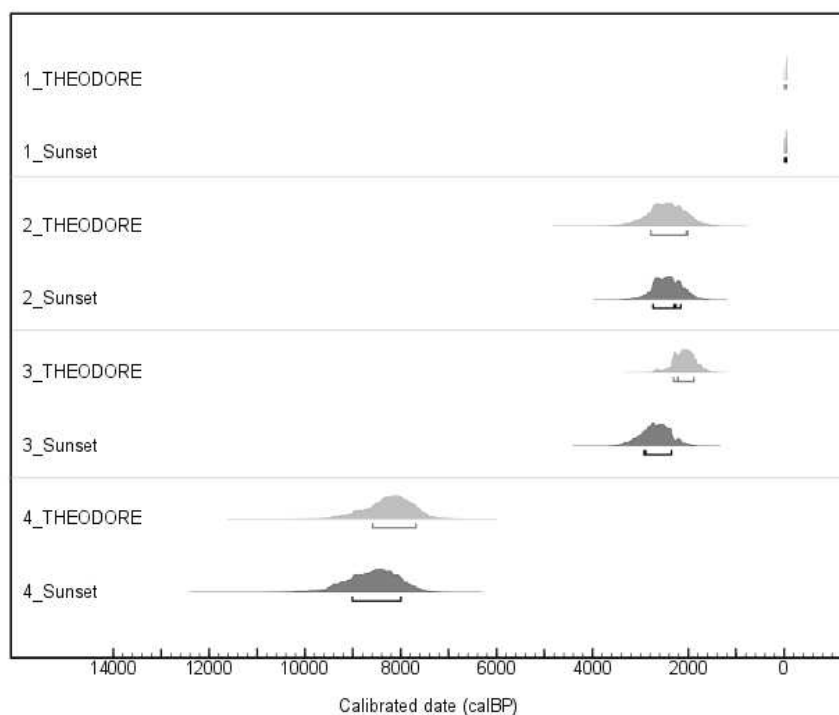
Figure 1: OxCal output for the compararability test for OC/EC separation using the THEODORE apparatus and the Sunset OC/EC analyzer directly coupled to the AMS. Bars below the age distributions indicate the 1 σ range. See Table 2 for the samples details.
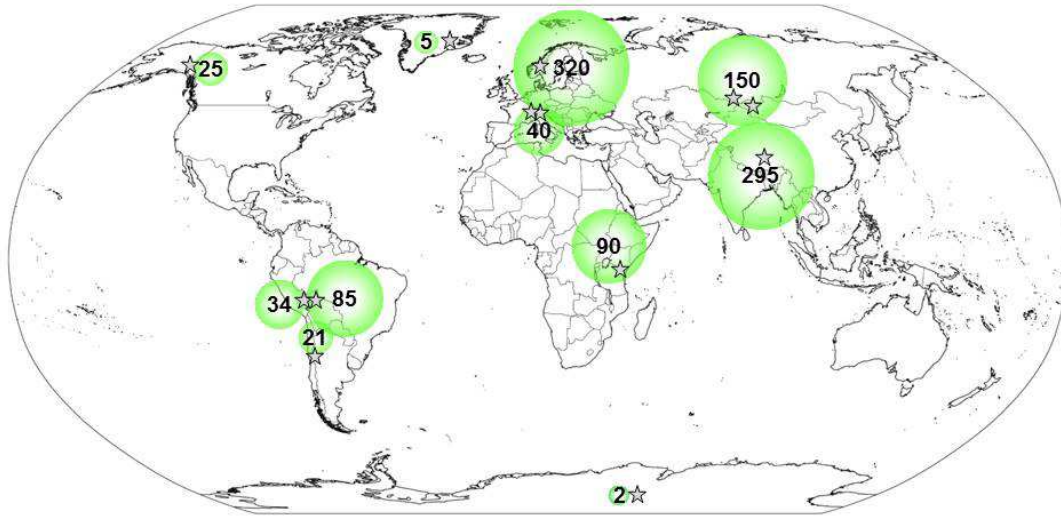
620

Figure 2: World map showing the sites from which ice samples were analysed with the ^{14}C method (gray stars): Edziza, Canada, 57.71° N 130.63° W; GRIP, Greenland, 72.59° N, 37.65° W, 3230 m a.s.l.; Juvfonne, Norway, 61.68 N, 8.35° E; Colle Gnifetti, Switzerland, 45.93° N, 7.87° E; Mt. Ortles, Italy, 46.51° N, 10.54° E; Belukha, Russia, 49.80° N, 86.55° E; Tsambagarav, Mongolia, 48.66° N, 90.86° E; Naimonanji, China 30.45° N, 81.54° E; Kilimanjaro, Tanzania, 3.06° S 37.34°

625 E; Quelccaya, Peru, 13.93° S, 70.83° W; Nevado Illimani, Bolivia, 16.03° S, 67.28° W; Mercedario, Argentina, 31.97° S, 70.12° W; Scharffenbergbotnen, Antartica, 74.00° S, 11.00° W. The average WIOC concentration in μg/kg at each site is indicated with green bubbles.
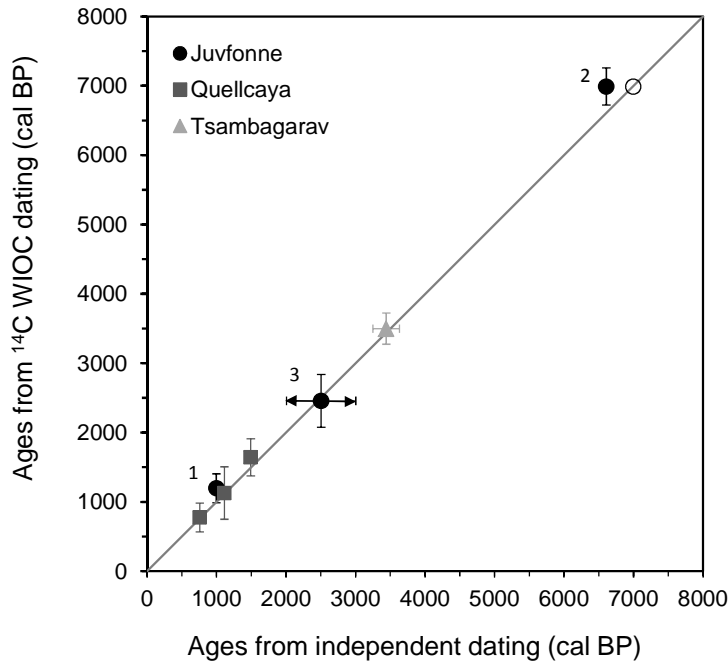
Figure 3: Scatter plot showing the ages obtained with the WIOC ^{14}C method for independently dated ice, including the conventionally ^{14}C dated Juvfonne organic-rich layers (Ødegård et al., 2016), the ^{14}C dated fly found in the Tsambagarav ice core, and the Quelccaya ice dated by annual layer counting (Thompson et al., 2013). Error bars denote the 1 σ uncertainty. Note that the Juvfonne WIOC samples and the organic-rich layers were not sampled from the exact same depth, but adjacent to each other. For the youngest (1) and oldest (2, containing the plant fragment) the ice for WIOC ^{14}C analysis was sampled

635 below the layers whereas the third sample (3) was bracketed by two layers. For (3) the arrow thus indicates the age range between the lower and upper 2σ boundary of these two layers, respectively. For (2) the open circle indicates an estimated age for the according WIOC ice sampling depth based on a fit through all the conventionally dated organic-rich layers, presented in Ødegård et al., 2016).

640

Figure 4: Photo of the fly found in segment 102 of the Tsambagarav ice core. The age of the fly was 3442±191 cal BP, while the surrounding ice yielded an age of 3495±225 cal BP (photo by Sandra Brügger).

645
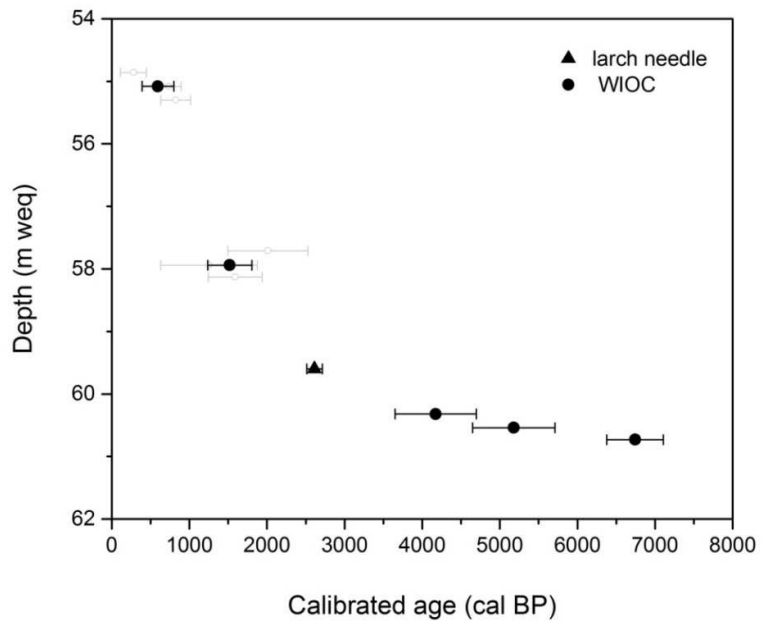
Figure 5: Dating of the bottom part of the Ortles ice core. Circles indicate the ages derived with the WIOC ^{14}C method and the triangle shows the age of the conventionally ^{14}C dated larch leaf found in the ice core (Gabrielli et al., 2016). Light grey circles show the ages obtained for the subsamples. Errors bars represent the 1 σ uncertainty.
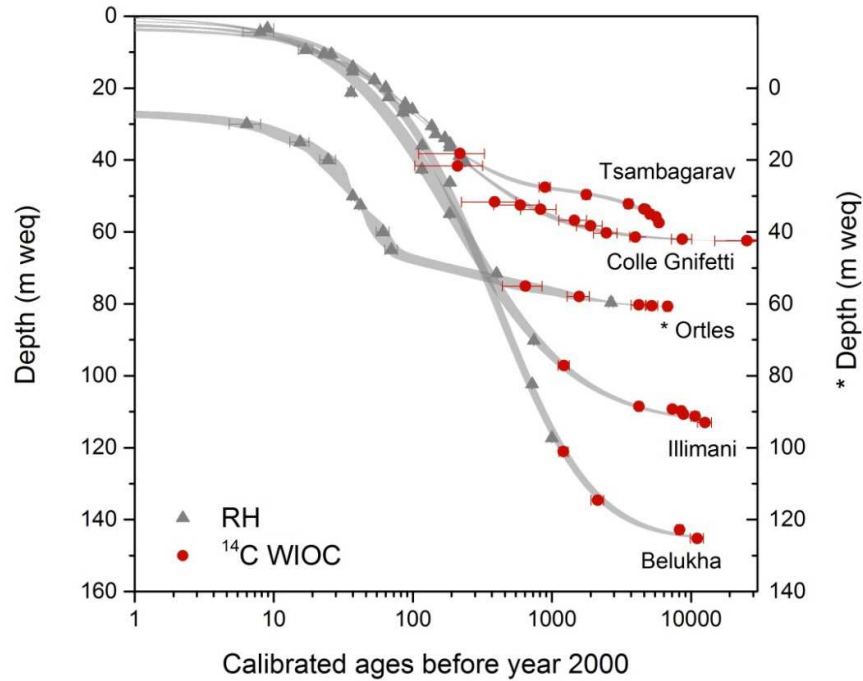
650

Figure 6: Compilation of age-depth relationships for five different ice cores, highlighting the importance of the WIOC ^{14}C dating to obtain continuous chronologies and to constrain the very specific glaciological conditions and settings of each site. For simplicity only reference horizons and ^{14}C dates were included. Gray triangles indicate reference horizons (RH) and red circles the ^{14}C-WIOC ages both plotted with 1σ uncertainties (smaller than the symbol size in some cases). For the Mt.
655   Ortles core ^{210}Pb dated horizons with a larger uncertainty were used as RH due to the lack of absolute time markers prior to 1958; the gray triangle at 57.8 m weq depth is the conventional ^{14}C age of the larch leaf. Gray shaded areas represent the 1σ range of the respective fit for retrieving a continuous age depth relationship. For sample details and the fitting approaches applied, see main text and Table 1. References to the original data are summarized in Table 1. Note that for better visibility (avoiding overlap with Tsambagarav and Colle Gnifetti) the curve for the Mt. Ortles glacier was shifted down by 20 m and
660   refers to the right-hand y-axis (*).